Journal of Microwaves, Optoelectronics and Electromagnetic Applications, Vol. 20, No. 3, September 2021
DOI: http://dx.doi.org/10.1590/2179-10742021v20i31137

A LiDAR Architecture Based on Indirect ToF For Autonomous Cars

Luis G. Da Silva and Arismar Cerqueira S. Jr.
Wireless and Optical Convergent Access Laboratory (WOCA), National Institute of Telecommunication (Inatel), Santa Rita do Sapucaí 3754000, Minas Gerais, Brazil
luis.gustavo@inatel.br and arismar@inatel.br

***Abstract*— A LiDAR architecture for autonomous cars is presented and validated by numerical and experimental results. The proposed scheme is based on indirect time-of-flight principle based on continuous-wave pseudorandom codes and incoherent detection for range evaluation. The range ambiguity and resolution are controlled by the parameters of the pseudorandom code. Experimental results are reported for target detection ranging from 13 to 1,000 m, as well as a demonstration of a dual-target detection, demonstrating the efficiency of the proposed LiDAR architecture to operate in real scenarios of autonomous cars. A measured range error of less than 0.6 % has been achieved for both single and dual-target detection.**

***Index Terms*—** Autonomous cars, incoherent detection, lidar, range finding.

I. INTRODUCTION

Recently, autonomous cars have been gained remarkable attention as a promising technology that might transform mobility with fully automated vehicles. Moreover, traffic improvements in both highway capacity and flow, guidance in unfamiliar locales and increase safety by collision avoidance systems are envisioned [1]. Navigation and control systems used to make decisions and judgments require external environment sensing with state-of-the-art neural networks to process and integrate data from a variety of sensors. To provide robustness and reliability to these systems it is necessary an arrangement of sensors including cameras, millimeter-wave radar, ultrasonic and laser radar, known as light detection and ranging (LiDAR) [2]. Each sensor has its applicability and LiDARs offer high angular resolution and distant 3-D data [3]. Nevertheless, reducing LiDARs' costs and extending its range and performance is a key challenge for autonomous cars [4].

Since the early 1960s the use of laser ranging systems have been reported in literature [5]. Therefore, LiDAR applications comprise target detection and ranging [6], target detection and ranging and velocity estimation [7], space and airborne laser scanning [8], [9], vibrometry [10], synthetic aperture imaging [11], chemical detection by gas absorption lines [12], wind sensor [13], three-dimensional images [14] and so on. LiDAR operation principle is similar to RADAR (radio detection and ranging), working as transmitting and receiving electromagnetic energy. Also, LiDAR operates in the optical frequency range collecting the backscattered light and provides superior angular resolution, higher directionality to solve small targets and low probability of interception [15]. Plenty

Brazilian Microwave and Optoelectronics Society-SBMO *received 25 Nov 2020; for review 21 Dec 2020; accepted 3 June 2021*
Brazilian Society of Electromagnetism-SBMag *ISSN 2179-1074*

of techniques for LiDAR range sensing have been proposed [15]-[20]. Most LiDARs applied to autonomous cars are based on the time-of-flight (ToF) principle, which might be categorized in indirect (i-ToF) or direct (d-ToF) according to the range calculation procedure [16]. The i-ToF technique uses the phase difference between periodic signals to determine targets distance [17]-[19] and d-ToF the round-trip time of a single, high peak power short pulse emission [16], [3].

An optical code division multiple access (CDMA) modulation scheme derived from optical orthogonal codes (OOC) was reported in [16] for automotive d-ToF systems. The influence of OOCs design parameters was evaluated and compared to standard single pulses transmission. In [17], a LiDAR architecture base on pseudorandom noise (PN) codes and periodic pulses modulation scheme was proposed to simultaneously determine the target range and speed. This was achieved by exploring the time-of-flight and Doppler effect principles. The authors in [18] presented a LiDAR and free-space optical communication system using a single architecture based on coherent detection. The LiDAR operation principle is similar to [17] with PN sequences and phase difference correlation for range measurement. In [19] Torun et al. proposed a multi-tone continuous-wave LiDAR with multiple fixed RF tones for range and speed information retrieval. Finally, LiDARs photonic integration circuits (PIC) technology have been proposed for cost and size reduction to realize chip-scale systems. An optical phased array (OPA) applied to autonomous cars LiDAR was designed, fabricated and characterized in [4]. Integrated OPAs with 2-D and 3-D LiDARs performance results were reported in [20].

In this paper, we propose and implement a LiDAR architecture for autonomous cars application based on indirect time-of-flight principle with continuous-wave pseudorandom codes and incoherent detection for range retrieval. Additionally, the proposed work is based on standard telecommunication components, allowing its use for detection and ranging application and data transmission for communication purposes as free-space optics (FSO) systems. Section II discusses the proposed LiDAR architecture and the obtained numerical results. An experimental setup has been conceived and evaluated as presented in Section III. Finally, conclusions and final comments are outlined in Section IV.

II. LIDAR OPERATION PRINCIPLE AND NUMERICAL RESULTS

A schematic of the proposed LiDAR architecture based on work in [18] is shown in Fig. 1. In summary, a continuous wave (CW) laser is modulated in amplitude by a pseudorandom code and transmitted to the target using a collimator or telescope lenses. The target reflected light is coupled into a fiber, photodetected and post-processed to obtain the target range information. The unambiguous range and resolution values depend on pseudorandom code parameters as bitrate and bit sequence duration. The LiDAR system might be divided into three main blocks named signal generator, signal receiver and signal processing. The signal generator block is formed by a CW laser source operating at 1550 nm, whose amplitude is externally modulated in a Mach-Zehnder modulator

Brazilian Microwave and Optoelectronics Society-SBMO received 25 Nov 2020; for review 21 Dec 2020; accepted 3 June 2021
Brazilian Society of Electromagnetism-SBMag *ISSN 2179-1074*

(MZM) biased at its quadrature point. A bit pattern generator (BPG) drives a pseudorandom bit sequence (PRBS) into MZM as a modulation signal. A sample of the PRBS signal is sent to the signal processing unit for the phase difference calculation step. The modulated laser light is then transmitted to the target. In the signal receiver section, a PIN photodiode converts the reflected light into an electrical signal which is amplified by a low noise amplifier (LNA). At the signal processing chain, the LNA output is digitized by an analog to digital converter (ADC) and post-processed with the PRBS sample to gather the range information.

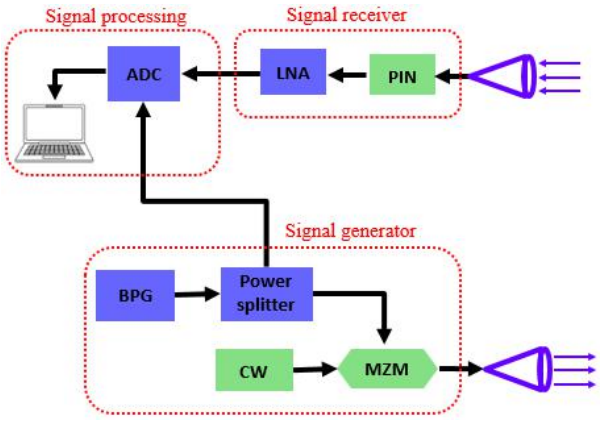

Fig. 1. Schematic of the proposed LiDAR system.

As the transmitted optical signal travels at the speed of light in the free-space, the relation between range distance R and round-trip time τ is given by:

$$R = c \times \frac{\tau}{2} \tag{1}$$

The round-trip time τ is determined by the cross-correlation between the PRBS sample and the processed backscattered optical signal. The cross-correlation peak gives the delay experienced by the target reflected signal. Besides, PRBS parameters define the range resolution and unambiguous range [18]. The range resolution ΔR is related to the PRBS bit rate, i.e., modulation bandwidth (BW), by:

$$\Delta R = \frac{c}{2 \times BW} \tag{2}$$

and the PRBS length multiplied by bit duration defines the repetition interval *RI*, which determines the unambiguous range R_{ua}.

$$R_{ua} = \frac{c \times RI}{2} \tag{3}$$

Numerical analysis has been performed in Optisystem® using the setup presented in Fig. 2. A CW laser operating at 1550 nm with 10 dBm output power is intensity-modulated by the PRBS signal in the MZM modulator, operating at its quadrature point. The PRBS bitrate is set to 1 Gbps and sequence length to 215-1 in the NRZ format. So then, the range resolution is equal to 15 cm with an unambiguous range of 4.9 km. The transmission channel is implemented by a free-space optics (FSO) and time delay blocks to emulate transmitted and reflected signals as a function of range. The received signal is photodetected by a PIN photodiode with InGaAs responsivity and amplified by an LNA with 15 dB of gain.

The signal processing step has been realized in Matlab® using the transmitted and received PRBS

ISSN 2179-1074

sequence as inputs. A calculation routine has been conceived to resolve the cross-correlation operation and establish the round-trip time τ. The range estimation as a function of cross-correlation level is obtained using (1). First, the setup in Fig. 2 is simulated for a range of 880 m. The transmitted and received PRBS sequence is analyzed in Matlab and the cross-correlation result is shown in Fig. 3(a). The cross-correlation peak is at 880.01 m, validating the proposed LiDAR architecture numerically. A scenario with two targets, i.e., two reflected signals, has also been analyzed. In this case, the transmitted signal is split into two branches and sent to two different delay paths equivalent to 400 and 880 m. In Fig. 3(b) is noticed two cross-correlation peaks at 400 and 880.01 m as expected. Therefore, the proposed LiDAR architecture has been numerically validated for single and dual-target detection conditions.

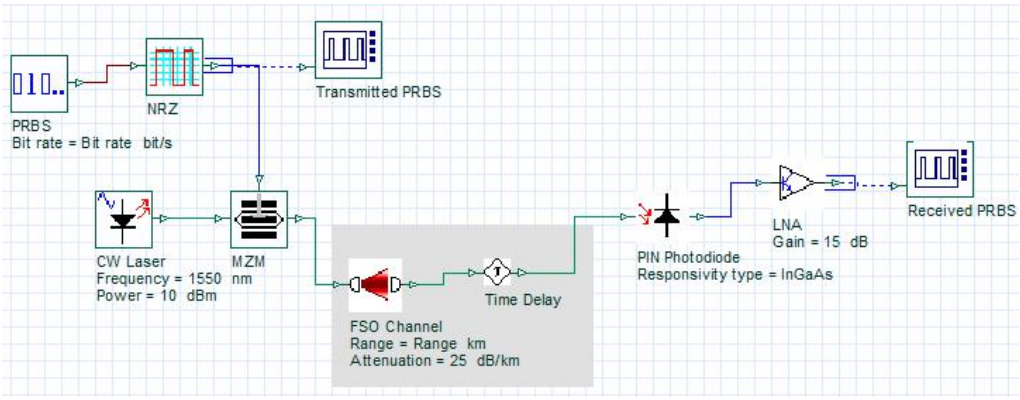

Fig. 2. Proposed LiDAR numerical setup.

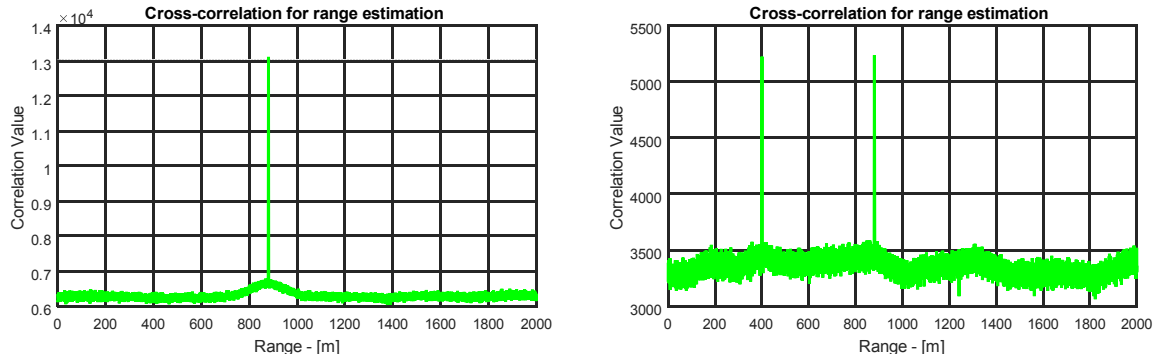

(a) (b)

Fig. 3. LiDAR numerical results. (a) Range estimation for 880 m. (b) Range estimation for 400 and 880 m.

III. EXPERIMENTAL RESULTS

The proposed LiDAR architecture has been experimentally implemented as shown in Fig. 4. The light source is a tunable C-band laser operating at 1550.12 nm with output power varying from 8 to 13 dBm. A pseudorandom bit sequence at 1 Gbps and 2^{15}-1 long is provided by a bit error tester (BERT) MP 2100B from Anritsu. The opto-electronic modulation stage is realized by a Fujitsu FTM7939EK 43 Gb/s single driver Mach-Zehnder modulator biased at its quadrature point with a fiber polarization controller (Thorlabs FPC031). For simplicity, the FSO link has been implemented at first with

ISSN 2179-1074

different single-mode fiber (SMF) spools to provide a known delay to the optical signal. At the receiver stage, a radio-over-fiber (RoF) module from Optical Zonu (OZ101) provides the PIN photodiode and 15 dB gain LNA amplifier. An optical power meter is placed at the RoF input for power safety control during the experiments. The RoF output is digitized by the Keysight DSAV084A oscilloscope operating at 5 GSa/s and 50 kpts. A PRBS sample is also digitized by this oscilloscope and used during the range calculation routine. Lastly, the oscilloscope waveforms are exported and applied to the Matlab range calculation routine for range estimation by cross-correlation values. The calculation routine is similar to the one used in the analysis of the numerical results. However, the propagation velocity in (1) has been replaced by the SMF fiber propagation velocity with a refractive index of 1.47.

Some measurements have been carried out with setup from Fig. 4 aiming to demonstrate its performance. First, a back-to-back measurement has been performed to evaluate the setup inherent delay. Fig. 5(a) reports the obtained setup delay with a cross-correlation peak at 6.98 m. Therefore, in the following results, this value is subtracted from the measurements to obtain only the SMF delay value. Applying an 880 m SMF spool in the LiDAR setup, the measured result is shown in Fig. 5(b). The obtained cross-correlation peak was at 880.36 m, representing a measured error of only 0.04 %.

Additionally, some patch cords and another SMF spool have also been tested and the obtained results are summarized in Table I. Different patch cords have been associated to gather lengths from about 13.4 to 23.7 m. The obtained patch cords lengths with LiDAR setup were 13.50, 18.60 and 23.70 m, whereas the error equal to 0.44, 0.1 and 0.08 %, respectively. These results corroborate to the proposed LiDAR applicability to also identify closer targets. Lastly, a 1,000 m SMF spool has been applied to the LiDAR setup giving rise to an estimated length of 998.42 m, i.e. an error of 0.15 %. In Table I, it is shown a comparison between the obtained results with the proposed LiDAR and a commercial optical time-domain reflectometer (OTDR).

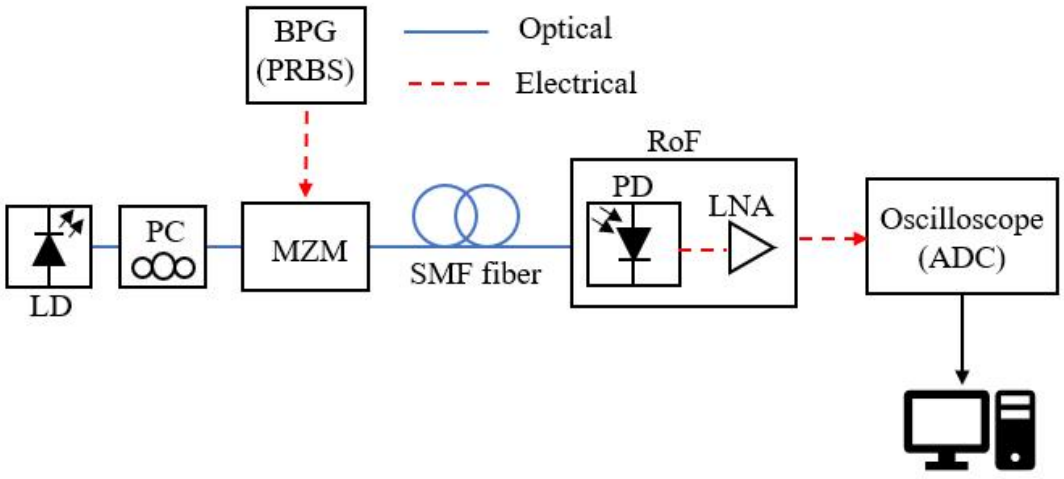

Fig. 4. Proposed LiDAR experimental setup.

Brazilian Microwave and Optoelectronics Society-SBMO *received 25 Nov 2020; for review 21 Dec 2020; accepted 3 June 2021*
Brazilian Society of Electromagnetism-SBMag *ISSN 2179-1074*

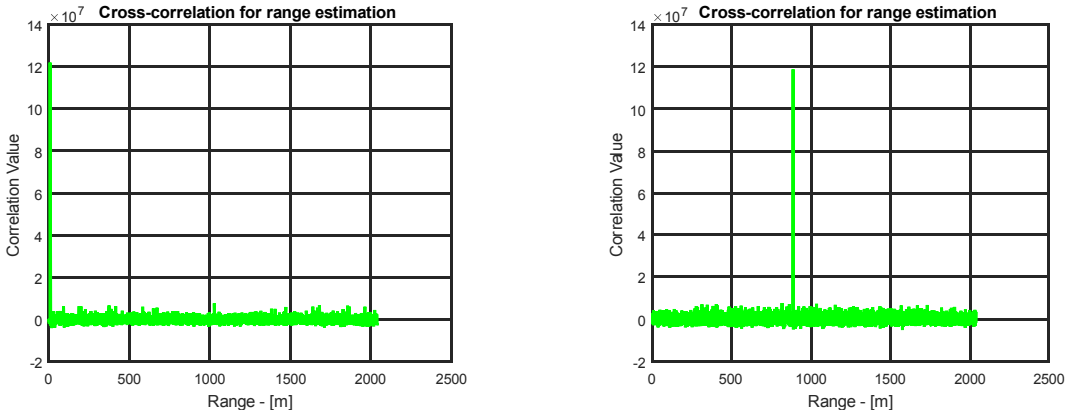

Fig. 5. LiDAR experimental results for single target. (a) B2B measurement. (b) Range estimation for 880 m SMF spool.

TABLE I. LIDAR MEASURED RESULTS FOR DIFFERENT TARGET DISTANCES

Sample	Length [m]	LiDAR [m]	OTDR [m]
Patch cord 1	13.44	13.50	–
Patch cord 2	18.58	18.60	–
Patch cord 3	23.72	23.70	–
SMF 1	880	880.36	880.90
SMF 2	1000	998.42	998.70

As numerically evaluated in the previous section, a dual-target condition has been conducted in the experimental setup. In this scenario, the transmitted signal is split into two branches by an optical splitter and two different paths are used to produce distinct delays. In the reception, these two different delayed signals are combined again by an optical combiner. The photodetected signal is digitized and analyzed as a single signal, but with two different delay information.

Again, a back-to-back measurement has been performed to account for the LiDAR system inherent delay, as presented in Fig. 6(a). A propagation delay equivalent to 16.48 m was obtained with this new setup due to the addition of optical splitter and combiner. In Fig. 6(b) are shown the LiDAR experimental results for the dual-target condition. The dual-target configuration has been implemented by an 880 m SMF spool as one transmission path and an 18.58 m patch cord arrangement for the second path. The cross-correlation results in Fig. 6(b) possess one peak value at 18.70 m and other at 880.22 m, validating the different delay detection. Under this condition, the range estimation error was 0.6 and 0.02 % for 18.58 and 880 m, respectively.

ISSN 2179-1074

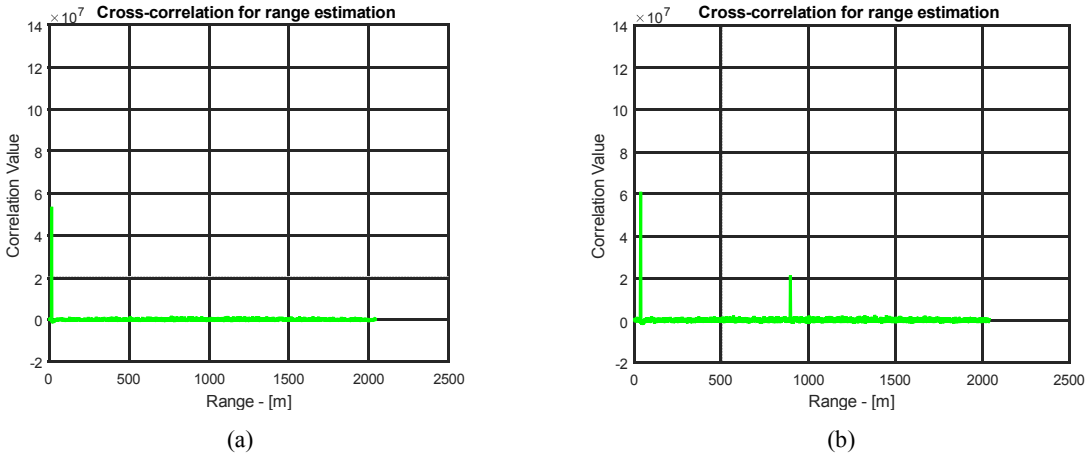

Fig. 6. LiDAR experimental results for dual target. (a) B2B measurement. (b) Range estimation for 880 m SMF spool and patch cords.

Table II summarizes the characteristics of the presented work related to reference works. The presented LiDAR architecture is based on telecommunication setup and components; therefore, it could be applied as an FSO system for communication purposes. In order to avoid high peak power short time pulse emission presented in conventional ToF, the proposed work presents a modulation code to retrieve the range information in a similar manner implemented by [16], [17], and [19]. However, the modulation technique implemented in [16] has the purpose of avoidance high peak power pulses and provide a coded system to improve its robustness, although the detection technique is direct ToF. The use of indirect ToF techniques and modulation codes have the ambiguity range characteristic, which can be controlled by modulation code parameters as a system variable. For autonomous car applications, besides ranging information, it is important to retrieve speed information as reported by [17] and [19] to provide an improved solution. Although the proposed architecture does not allow gathering the speed information, it is possible to implement this feature by modifying the schematic shown in Fig. 1 as presented by [16].

TABLE II. COMPARISON AMONG LIDAR ARCHITECTURES

Ref.	Application	Detection technique	Ambiguity range	Resolution	Additional feature
[16]	Detection and ranging	Direct ToF	Code weight and size dependent	Not specified	Use of CDMA for robustness
[17]	Detection and ranging + Speed	Indirect ToF	Not specified	Not specified	Speed measurement by Doppler effect
[19]	Detection and ranging + Speed	Indirect ToF	Number of RF tones	< 1cm	Speed measurement by RF tones amplitude
This work	Detection and ranging	Indirect ToF	PRBS dependent	< 6cm	FSO implementation

ISSN 2179-1074

IV. CONCLUSIONS

It has been presented a LiDAR architecture for detection and ranging based on indirect time-of-flight implemented by modulation codes with pseudorandom bit sequences, eliminating the need for high peak power short time pulse emission. Besides, the proposed LiDAR architecture is based on telecommunication setup and it is possible to extend its use for communication purposes by means of an FSO system. Regarding its application, the proposed work might be used in autonomous car scenarios as an alternative for detection and ranging implementation. Additionally, the proposed architecture can be modified and updated to retrieve speed information from the measured data.

Numerical simulations and experiments have been carried out in a controlled environment to demonstrate the efficiency of the proposed LiDAR architecture. In this manner, the proposed work has been evaluated for targets ranging from 13 to 1,000 m using single-mode fibers as a propagation medium. Additionally, single and dual-target detection have been reported with a measurement error of less than 0.6 %. Future works regard the implementation of experiments with free-space optics using collimators and plano-convex spherical lenses for optical signal transmission and reception.

ACKNOWLEDGMENTS

This work was partially supported by RNP, with resources from MCTIC, Grant No. No 01245.010604/2020-14, under the 6G Mobile Communications Systems project of the Radiocommunication Reference Center (Centro de Referência em Radiocomunicações - CRR) of the National Institute of Telecommunications (Instituto Nacional de Telecomunicações - Inatel), Brazil. The authors also thank the financial support from CNPq, CAPES, FINEP, RNP and FAPEMIG.

REFERENCES

[1] T. Luettel, M. Himmelsbach and H. Wuensche, "Autonomous Ground Vehicles—Concepts and a Path to the Future," in *Proceedings of the IEEE*, vol. 100, no. Special Centennial Issue, pp. 1831-1839, 13 May 2012.
[2] J. Hecht, "Lidar for Self-Driving Cars," in *Optics & Photonics News*, vol. 29, no. 1, pp. 26-33, 2018.
[3] J. Liu, Q. Sun, Z. Fan and Y. Jia, "TOF Lidar Development in Autonomous Vehicle," *2018 IEEE 3rd Optoelectronics Global Conference (OGC)*, Shenzhen, 2018, pp. 185-190.
[4] W. Xie, T. Komljenovic, J. Huang, M. Tran, M. Davenport, A. Torres, P. Pintus, and J. Bowers, "Heterogeneous silicon photonics sensing for autonomous cars [Invited]," in *Opt. Express*, vol. 27, no. 3, pp. 3642-3663, 2019.
[5] R. D. Richmond and S. C. Cain, *Direct-Detection LADAR Systems*. SPIE Press, 2010.
[6] M. C. Amman, T. B. M. Lescure, R. Myllyla, and M. Rioux, "Laser ranging: a critical review of usual techniques for distance measurement," in *Opt. Eng.*, vol. 40, vol. 1, pp. 10–19, Jan. 2001.
[7] A. Martin *et al*., "Photonic Integrated Circuit-Based FMCW Coherent LiDAR," in *Journal of Lightwave Technology*, vol. 36, no. 19, pp. 4640-4645, Oct.1, 2018.
[8] P. Daukantas, "Lidar in Space: From Apollo to the 21st Century," in *Optics & Photonics News*, vol. 20, vol. 6, pp. 30-35, 2009.
[9] C. Mallet and F. Bretar, "Full-waveform topographic lidar: State-of-the-art, " in *ISPRS Journal of Photogrammetry and Remote Sensing*, vol. 64, no. 1, pp. 1-16, Jan. 2009.
[10] P. Lutzmann, B. Göhler, F. van Putten, and C. A. Hill, "Laser vibration sensing: Overview and applications," in *Proc. SPIE 8186*, 2011.
[11] W. Buell, N. Marechal, J. Buck, R. Dickinson, D. Kozlowski, T.Wright, and S. Beck, "Demonstrations of synthetic aperture imaging ladar," in *Proc. SPIE 5791*, pp. 152–166, 2005.
[12] S. Boudreau, S. Levasseur, C. Perilla, S. Roy, and J. Genest, "Chemical detection with hyperspectral lidar using dual frequency combs," in *Opt. Express*, vol. 21, no. 6, pp. 7411–7418, 2013.
[13] S. Kameyama, T. Ando, K. Asaka, Y. Hirano, and S. Wadaka, "Compact all-fiber pulsed coherent Doppler lidar system for wind sensing," in *Appl.Opt.*, vol. 46, no. 11, pp. 1953–1962, 2007.
[14] P. F. McManamon, "Review of ladar: a historic, yet emerging, sensor technology with rich phenomenology," in *Opt. Eng.*, vol. 51, no. 6, pp. 060901, 2012.

received 25 Nov 2020; for review 21 Dec 2020; accepted 3 June 2021

ISSN 2179-1074

[15] D. Onori, F. Scotti, M. Scaffardi, A. Bogoni and F. Laghezza, "Coherent Interferometric Dual-Frequency Laser Radar for Precise Range/Doppler Measurement," in *Journal of Lightwave Technology*, vol. 34, no. 20, pp. 4828-4834, Oct.15, 2016.
[16] T. Fersch, R. Weigel and A. Koelpin, "A CDMA Modulation Technique for Automotive Time-of-Flight LiDAR Systems," in *IEEE Sensors Journal*, vol. 17, no. 11, pp. 3507-3516, June, 2017.
[17] X. Mao, D. Inoue, S. Kato and M. Kagami, "Amplitude-Modulated Laser Radar for Range and Speed Measurement in Car Applications," in *IEEE Transactions on Intelligent Transportation Systems*, vol. 13, no. 1, pp. 408-413, March 2012.
[18] F. Scotti *et. al*., "Dual use architecture for innovative lidar and free space optical communications," in *Appl. Opt.*, vol. 56, no. 31, pp. 8811-8815, 2017.
[19] R. Torun, M. M. Bayer, I. U. Zaman, J. E. Velazco and O. Boyraz, "Realization of Multitone Continuous Wave Lidar," in *IEEE Photonics Journal*, vol. 11, no. 4, pp. 1-10, Aug. 2019, Art no. 5501910.
[20] C. V. Poulton *et al*., "Long-Range LiDAR and Free-Space Data Communication With High-Performance Optical Phased Arrays," in *IEEE Journal of Selected Topics in Quantum Electronics*, vol. 25, no. 5, pp. 1-8, Sept.-Oct. 2019, Art no. 7700108.

received 25 Nov 2020; for review 21 Dec 2020; accepted 3 June 2021

ISSN 2179-1074